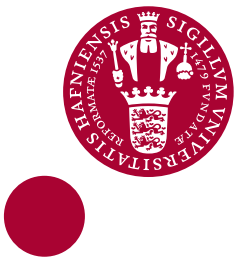

Maternal Antibodies Inhibit Neonatal and Infant Responses to Vaccination by Shaping the Early-Life B Cell Repertoire within Germinal Centers

Vono, Maria; Eberhardt, Christiane Sigrid; Auderset, Floriane; Mastelic-Gavillet, Beatris; Lemeille, Sylvain; Christensen, Dennis; Andersen, Peter; Lambert, Paul Henri; Siegrist, Claire Anne

Published in:
Cell Reports

DOI:
10.1016/j.celrep.2019.07.047

Publication date:
2019

Document version
Publisher's PDF, also known as Version of record

Article

Cell Reports

Maternal Antibodies Inhibit Neonatal and Infant Responses to Vaccination by Shaping the Early-Life B Cell Repertoire within Germinal Centers

Graphical Abstract

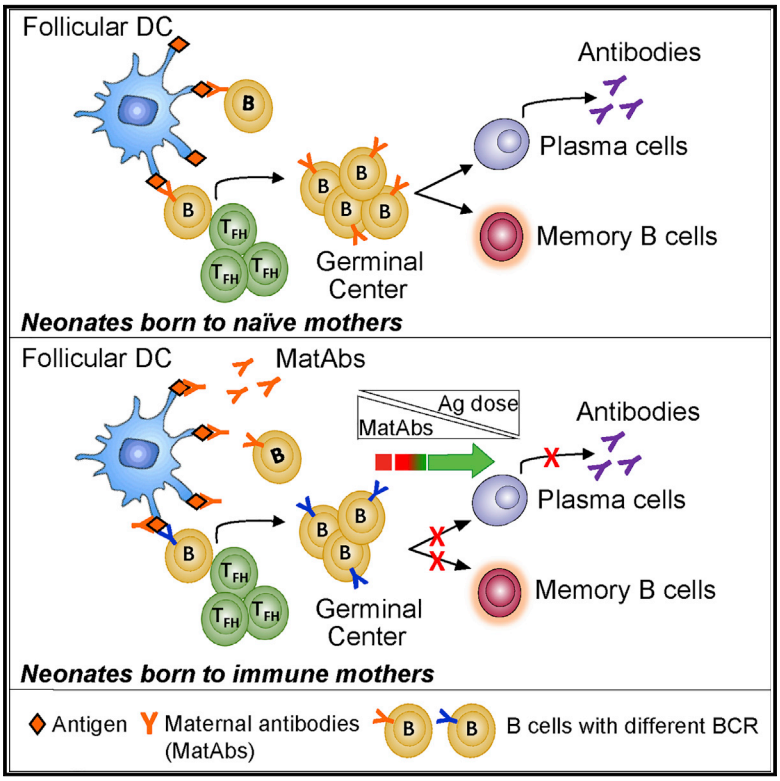

Highlights

- MatAbs inhibit early-life antibody responses but do not prevent B cell activation
- Germinal center formation occurs despite MatAbs, but their output is altered
- Plasma cell and memory B cell differentiation is affected in a titer-dependent manner
- GC B cells elicited in the presence or absence of MatAbs express distinct BCRs

Authors

Maria Vono, Christiane Sigrid Eberhardt, Floriane Auderset, ..., Peter Andersen, Paul-Henri Lambert, Claire-Anne Siegrist

Correspondence

maria.vono@unige.ch

In Brief

Maternal antibodies (MatAbs) protect offspring from infections but limit their vaccine responses through still poorly known mechanisms. Vono et al. report that MatAbs do not prevent B cell activation or germinal center formation but control plasma cell and memory B cell differentiation, shaping the long-term antigen-specific B cell repertoire.

Vono et al., 2019, Cell Reports *28*, 1773–1784
August 13, 2019
https://doi.org/10.1016/j.celrep.2019.07.047

CellPress

Cell Reports
Article

Maternal Antibodies Inhibit Neonatal and Infant Responses to Vaccination by Shaping the Early-Life B Cell Repertoire within Germinal Centers

Maria Vono,[1,6,*] Christiane Sigrid Eberhardt,[1] Floriane Auderset,[1] Beatris Mastelic-Gavillet,[1,5] Sylvain Lemeille,[2] Dennis Christensen,[3] Peter Andersen,[3,4] Paul-Henri Lambert,[1] and Claire-Anne Siegrist[1]
[1]WHO Collaborative Center for Vaccine Immunology, Department of Pathology and Immunology, University of Geneva, Geneva 1211, Switzerland
[2]Department of Pathology and Immunology, University of Geneva, Geneva 1211, Switzerland
[3]Vaccine Adjuvant Research, Department of Infectious Disease Immunology, Statens Serum Institut, Copenhagen 2300, Denmark
[4]Department of Immunology and Microbiology, University of Copenhagen, Copenhagen, 2300, Denmark
[5]Present address: Center for Experimental Therapeutics, Ludwig Center for Cancer Research, Department of Oncology, University of Lausanne, Lausanne, 1011, Switzerland
[6]Lead Contact
*Correspondence: maria.vono@unige.ch
https://doi.org/10.1016/j.celrep.2019.07.047

SUMMARY

Maternal antibodies (MatAbs) protect offspring from infections but limit their responses to vaccination. The mechanisms of this inhibition are still debated. Using murine early-life immunization models mimicking the condition prevailing in humans, we observed the induction of CD4-T, T follicular helper, and germinal center (GC) B cell responses even when early-life antibody responses were abrogated by MatAbs. GC B cells induced in the presence of MatAbs form GC structures and exhibit canonical GC changes in gene expression but fail to differentiate into plasma cells and/or memory B cells in a MatAb titer-dependent manner. Furthermore, GC B cells elicited in the presence or absence of MatAbs use different V_H and V_k genes and show differences in genes associated with B cell differentiation and isotype switching. Thus, MatAbs do not prevent B cell activation but control the output of the GC reaction both quantitatively and qualitatively, shaping the antigen-specific B cell repertoire.

INTRODUCTION

The toll of infectious diseases is at its highest during the first year of life (Bhutta and Black, 2013), a period of vulnerability that may be mitigated by the presence of antibodies of maternal origin. Seroprotection may be achieved or enhanced by maternal immunization inducing or increasing maternal antibody (MatAb) titers and, thus, their subsequent transplacental transfer to the offspring (Edwards, 2015). The positive effect of this intervention is demonstrated by the reduction in infant hospitalization and death following maternal immunization against tetanus, influenza, and pertussis (Benowitz et al., 2010; Kachikis and Englund, 2016), whereas novel maternal vaccines against respiratory syncytial virus (RSV) (Mazur et al., 2018) and group B *Streptococcus* (Lin et al., 2018) are in advanced clinical development.

Numerous studies, including recent ones (Jones et al., 2014), have reported dampening or inhibition of antibody responses in infants of immunized mothers (Kurikka et al., 1995; Englund et al., 1995; Borràs et al., 2012; Maertens et al., 2017), and it is therefore essential to assess the long-term effect of maternal immunization on the early-life immune system (Giles et al., 2018). Maternal immunization against *S. pneumoniae* was even associated with increased risk of otitis media in the first 6 months of life despite infant immunization at 2 and 4 months (Daly et al., 2014).

The mechanisms of inhibition of responses to immunization by MatAbs are still debated. Twenty years ago, total $CD4^+$ T cell responses were described as being largely unaffected (Siegrist et al., 1998a, 1998b) even when antibody responses were fully inhibited by MatAbs. It was postulated that B cell responses were inhibited mainly by (1) antigen neutralization (live replicating vaccines); (2) epitope masking preventing antigen binding and, thus, infant B cell priming (as in antibody feedback regulation studies) (Brüggemann and Rajewsky, 1982; Heyman and Wigzell, 1984); (3) active inhibition of infant B cell activation by Fcγ receptor IIB (FcγRIIB)-mediated signaling (Kim et al., 2011; Edwards, 2015); and (4) clearance of MatAb-coated vaccine antigens through Fc-dependent phagocytosis (Siegrist, 2003).

In contrast to all of these hypotheses, we show here that even high MatAb titers do not prevent neonatal B cell activation or their differentiation in germinal center (GC) B cells following vaccination but that they subsequently affect GC B cell differentiation into plasma cells (PCs) and memory B cells (MBCs), imposing significant differences in their V_H and V_k gene usage. Thus, MatAbs exert their influence on neonatal and infant B cell responses both quantitatively and qualitatively by shaping the GC output and the antigen-specific B cell repertoire.

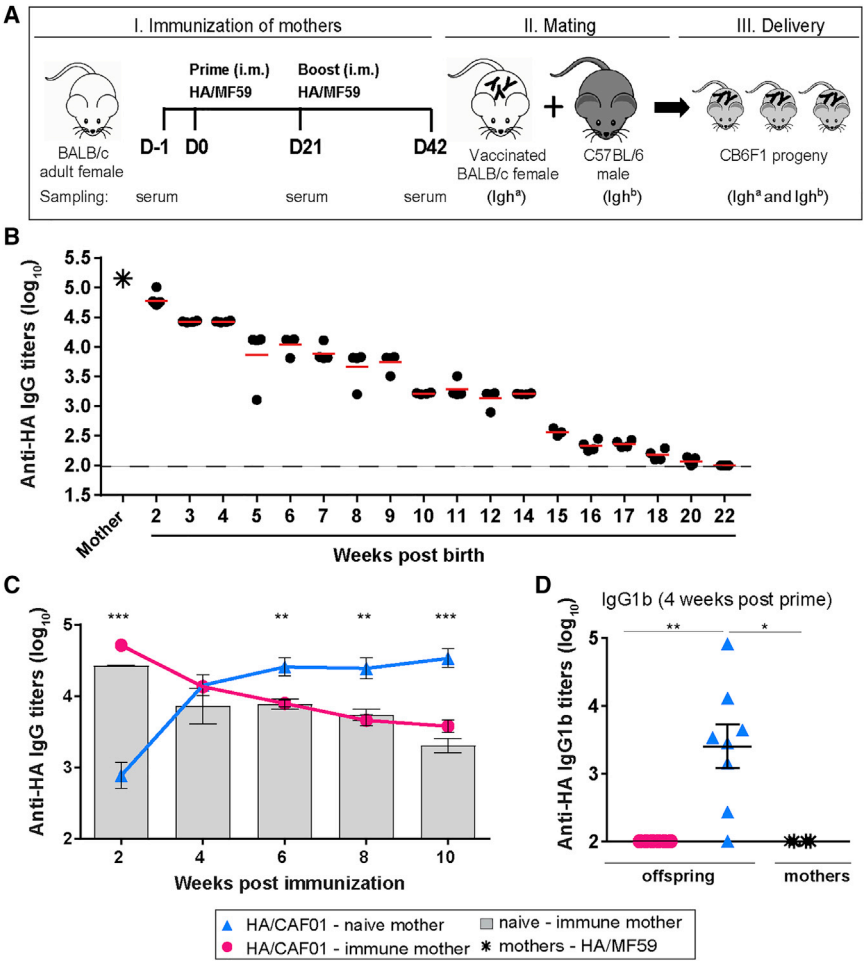

Figure 1. High Titers of Antigen-Specific Maternal Antibodies Inhibit Neonatal Antibody Responses to Vaccination

(A) Schematic representation of the experimental model. BALB/c females received two doses of HA/MF59 intramuscularly (i.m.) on days 0 (prime) and 21 (boost). 3 weeks post-boost, vaccinated or unimmunized (controls) females were mated with C57BL/6J males to generate CB6F1 offspring.

(B) Kinetics of the waning of HA-specific IgG maternal antibodies in naive CB6F1 pups from HA/MF59-immunized mothers; dots show values per individual mouse, whereas red lines indicate means. Data are from one representative experiment.

(C and D) Neonates born to HA/MF59-immunized (immune mother) or naive control mothers were vaccinated at 1 week of age with HA/CAF01. Non-immunized pups from immune mothers served as a control group. Data are representative of at least two independent experiments. Mann-Whitney *U* test: $^{*}p < 0.05$, $^{**}p < 0.01$, $^{***}p < 0.001$.

(C) HA-specific IgG titers post immunization. Values represent mean logarithmic titers (log10) of at least six mice per group ± SEM. Statistics show significant differences between HA/CAF01-immunized pups from immune and naive mothers.

(D) Serum HA-specific IgG1b titers 4 weeks after neonatal immunization (or in immune BALB/c mothers). Dots show values per individual mouse, whereas lines indicate means ± SEM; n = 4–7 mice/group.

RESULTS

High Titers of Antigen-Specific Maternal Antibodies Inhibit Neonatal and Infant Antibody Responses to Vaccination

We developed a first model of MatAb transfer in which BALB/c female mice (Igh^a) received two doses of a monovalent influenza hemagglutinin (HA)-based vaccine adjuvanted with MF59 (HA/MF59) to induce very high HA-specific immunoglobulin G (IgG) titers (on average, 5.0 log10 3 weeks post-boost) and were subsequently mated with C57BL/6J males (Igh^b) to generate CB6F1 offspring expressing both Igh^a and Igh^b antibodies (Figure 1A). This allowed discriminating MatAbs from the antibodies generated by neonatal immunization. In the first 2 weeks of age, HA-specific IgG titers were similarly high in the offspring as in their mother (Figure 1B). In the offspring, MatAbs declined steadily over time, persisting for up to 20 weeks after birth (Figure 1B).

To elicit strong neonatal responses to influenza HA, we used the CAF01 adjuvant (Vono et al., 2018). Neonatal (1-week-old) mice born to influenza-immune or -naive (control) mothers received one dose of HA/CAF01 (or were left unimmunized as controls), and HA-specific IgG titers were measured regularly after immunization. High and sustained HA-specific antibody responses were detected in immunized neonates from naive mothers (Figure 1C), as reported previously (Vono et al., 2018). In contrast, active immunization did not induce antibody responses in the offspring of immune mothers; HA-specific IgG titers remained similar in HA/CAF01-vaccinated and naive control pups from immune mothers (Figure 1C). Because HA/CAF01 primarily induces IgG1 antibodies (Vono et al., 2018), we measured HA-specific $IgG_1{}^b$ antibodies, which were only observed in pups born to naive mothers (Figure 1D). Postponing immunization until the age of 3 weeks (infant mice), when HA-specific IgG antibodies were 5-fold lower (4.5 log10), was not yet sufficient to elicit antibody responses to HA/CAF01 (Figure S1). This confirmed that high levels of HA-specific MatAbs fully inhibited early-life antibody responses to HA/CAF01.

Maternal Antibodies Do Not Affect Total $CD4^+$ T Cell Responses but Limit the Expansion of T Follicular Helper (T_{FH}) Cells

Total $CD4^+$ T helper (Th) cell responses were reported as being unaffected even in the presence of MatAb levels that completely inhibited antibody responses (Siegrist et al., 1998a; Weeratna et al., 2001; Crowe et al., 2001). Accordingly, HA/CAF01 immunization induced similar HA-specific $CD4^+$ T cell responses

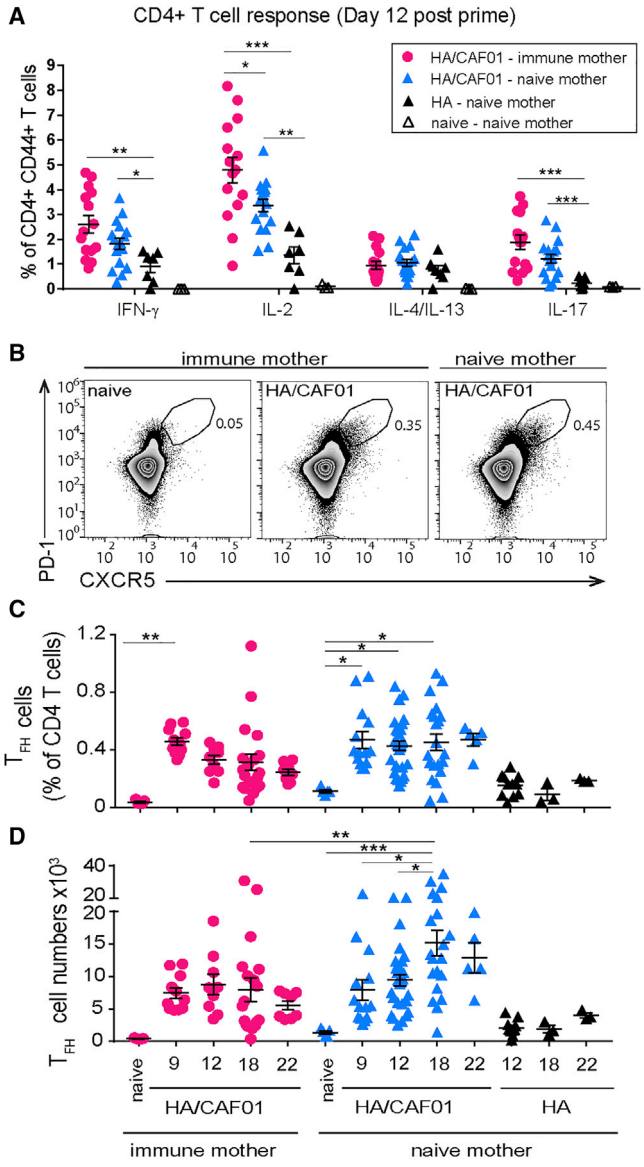

Figure 2. Maternal Antibodies Do Not Affect Total CD4⁺ T Cell Responses but Limit the Expansion of T_{FH} Cells

(A–D) 1-week-old CB6F1 mice born to HA/MF59-immunized or naive mothers were vaccinated (or not) with a single dose of HA/CAF01. Groups of neonates from naive mothers received HA/PBS as an additional control.

(A) Spleens were harvested on day 12 after immunization, and HA-specific $CD4^+$ Th cells were reactivated *in vitro* with HA prior to intracellular cytokine staining and flow cytometric analysis. The graph shows proportions of $CD4^+CD44^+$ HA-specific cytokine-expressing T cells.

(B–D) On the indicated days after immunization, dLNs were harvested to quantify T_{FH} cells by flow cytometry. Shown are representative plots showing $CXCR5^{high}PD\text{-}1^{high}$ T_{FH} cells among $CD4^+$ T cells (B). Graphs report the frequencies (C) and the numbers (D) of T_{FH} cells. Naive mice from both groups served as controls.

(A, C, and D) Dots show values per individual mouse, whereas black lines indicate means ± SEM; $n \geq 3$ mice/group. Data were pooled from at least two independent experiments per time point. *$p < 0.05$, **$p < 0.01$, ***$p < 0.001$; Mann-Whitney *U* test, all immunized groups significantly differed from naive control mice (not shown in the graph) (A); one-way ANOVA (statistics between CAF01-adjuvanted and unadjuvanted groups from naive mothers are not shown in the graph) (C and D).

with a predominant Th1/Th17 profile in pups of HA-immunized or naive mothers. Frequencies of $CD4^+CD44^+$ T cells secreting interleukin-2 (IL-2) but not other cytokines were even higher in the offspring of immune mothers (Figure 2A).

T_{FH} cells are specialized providers of T cell help to B cells and, thus, essential for GC formation, affinity maturation, somatic mutation, and development of high-affinity antibodies, PCs, and MBCs (Crotty, 2011; Vinuesa et al., 2010). We thus measured the frequencies and numbers of T_{FH} cells in the draining lymph nodes (dLNs) of immunized pups by flow cytometry. T_{FH} cells were defined as $CD4^+$ $CXCR5^{high}PD\text{-}1^{high}$ cells and gated as shown in Figure 2B. As reported previously (Vono et al., 2018), HA/CAF01 induced strong T_{FH} cell responses in neonates of naive mothers, with sustained frequencies up to day 22 (Figure 2C) and increasing numbers reaching a plateau on day 18 after immunization (Figure 2D). T_{FH} cells were also induced in the offspring of HA/MF59-immunized mothers but with different kinetics; T_{FH} cell frequencies peaked on day 9 after immunization, at similar frequencies as in control pups, but a decreasing trend was observed over time (Figure 2C). T_{FH} cell numbers did not increase between days 9 and 22, remaining significantly lower in pups of immunized than naive mothers (Figure 2D). The T_{FH} cell gated population highly expressed Bcl6, independent of the presence of MatAbs (Figure S2). Administration of CAF01 without HA did not elicit T_{FH} cell responses (Figure S3A).

Thus, although total $CD4^+$ T cell responses were not affected by the presence of high levels of MatAbs, they did not prevent induction but limited the expansion of T_{FH} cells.

High Levels of Maternal Antibodies Do Not Prevent Induction of GC B Cells Post-Vaccination but Limit Their Expansion

A single dose of HA/CAF01 induced potent GC B cell responses in pups of naive mothers (Vono et al., 2018). Here we measured $B220^+GL7^+FAS^+$ GC B cells elicited by HA/CAF01 in the dLNs of pups born to HA/MF59-immunized mothers (Figures 3A–3C). Neonates immunized with HA/PBS or non-immunized served as negative controls. As an additional specificity control, we verified that CAF01 administered without HA did not elicit GC B cell responses (Figure S3B).

Unexpectedly, given the lack of antibody responses (Figures 1C and 1D), HA/CAF01 immunization did elicit GC B cells even in pups born with high MatAb titers; GC B cells were detected on day 9 in both groups, increasing until day 18. However, on days 12 and 18, GC B cell frequencies (Figure 3B) and numbers (Figure 3C) remained significantly lower in pups of immune mothers than in pups of naive mothers. To confirm that these GC B cells were organized in *bona fide* GC structures, we imaged follicular B cells (IgD, green) and GC B cells (peanut agglutinin [PNA], red) in sections of the dLNs. On days 12 (Figure 3D) and 18 (data not shown), well-organized GC structures were observed even in HA/CAF01-immunized pups born to immune mothers.

We next used biotin-labeled HA and fluorochrome-conjugated streptavidin to estimate the proportion of HA-binding GC B cells,

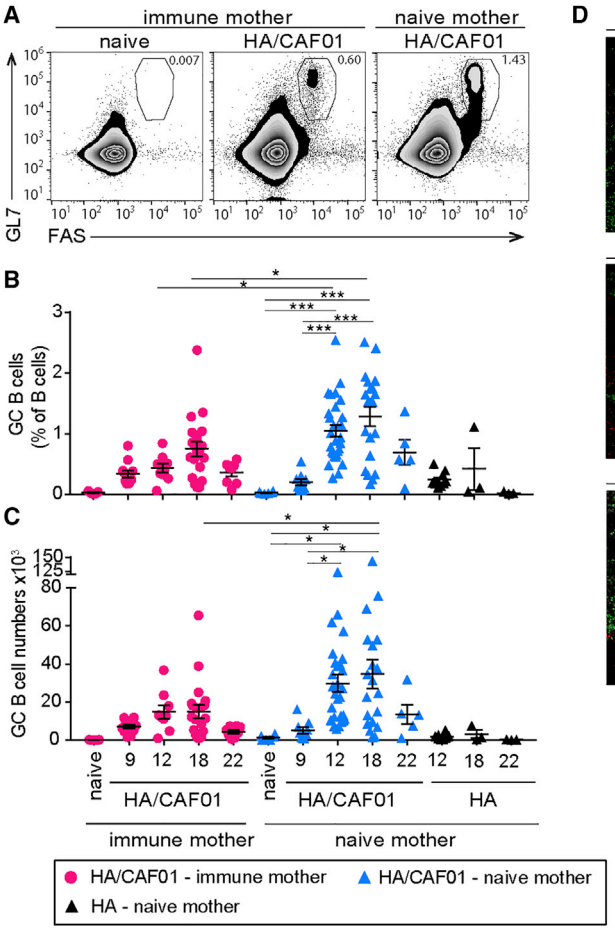

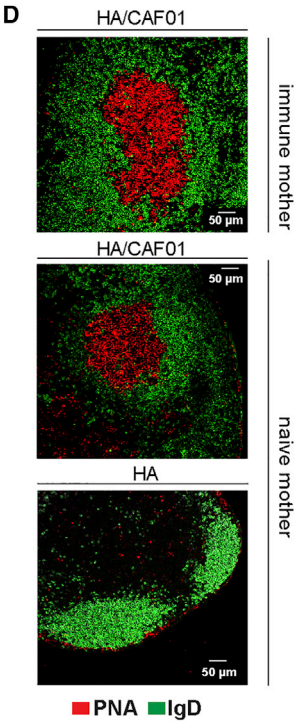

Figure 3. High Levels of Maternal Antibodies Do Not Prevent Induction of GC B Cells after Vaccination but Limit Their Expansion

(A–D) Neonates born to HA/MF59-immunized or naive mothers were vaccinated with HA/CAF01 or left unimmunized. Groups of neonates born to naive control mothers received HA/PBS as an additional control.

(A–C) Draining LNs were harvested at the indicated time points after immunization, and samples were analyzed by flow cytometry. Representative plots show the frequencies of $GL7^+FAS^+$ GC B cells among $B220^+$ B cells on day 18 after immunization (A). Graphs report the frequencies (B) and the numbers (C) of GC B cells over time for the indicated conditions. Naive mice from both groups served as negative controls. Dots show values per individual mouse, whereas black lines indicate means ± SEM. Data were pooled from at least two independent experiments per time point. Statistics between CAF01-adjuvanted and unadjuvanted groups from naive mothers are not shown in the graph. One-way ANOVA: $^*p < 0.05$, $^{***}p < 0.001$.

(D) Representative sections of dLNs showing immunohistochemical staining for IgD (green) and the peanut agglutinin (PNA, red) GC marker; GC B cells are IgD^-PNA^+. n ≥ 3 mice/group for all experiments.

which was technically challenging given the low number of GC B cells following neonatal immunization. We observed an average of 20% of HA-binding GC B cells independent of the presence or absence of MatAbs (Figures 4A and 4B). However, we demonstrated that, at the peak of GC responses (day 18 after immunization), total GC B cell frequencies correlate linearly with HA-specific IgG antibody responses in neonates born to naive mothers (Figure 4C).

To exclude the influence of other components transferred to the offspring through maternal milk, we adoptively transferred HA-immune serum in naive neonates 24 h prior to HA/CAF01 immunization. This generated the same observations as HA/CAF01 immunization in pups of immune mothers (data not shown).

Thus, even very high MatAb titers, which prevent induction of any detectable antibody response, do not preclude induction of GC B cells but limit their expansion.

High Titers of Maternal Antibodies Prevent GC B Cell Differentiation toward PCs and MBCs

Within the GC reaction, B cells either die or further differentiate into PCs or MBCs. We thus investigated the effect of MatAbs on GC B cell differentiation toward PCs and MBCs.

Cells with the $B220^{int/low}CXCR4^+CD138^+$ PC phenotype were quantitated by flow cytometry in dLNs on days 9, 12, 18, and 22 after HA/CAF01 neonatal vaccination (Figures 5A and 5B; data not shown). PCs were few, detectable only on day 18 after HA/CAF01 immunization in pups of naive mothers (Figures 5A and 5B). PCs egress from lymph nodes (LNs), and homing to the bone marrow (BM) is critical for their long-term survival, whereas other GC B cells develop into MBCs. We thus measured PCs in the BM and spleen (control) and MBCs in the spleen by enzyme-linked immunospot (ELISpot) assay 10 weeks after HA/CAF01 immunization. We observed low but consistent frequencies of PCs and MBCs in immunized pups of control mothers. In contrast, neither PCs nor MBCs were observed in the HA/CAF01-immunized offspring of immune mothers (Figures 5C and 5D).

To obtain further evidence of B cell differentiation toward MBCs, mice were boosted with HA/PBS 14 weeks after HA/CAF01 priming, and their B cell recall responses were characterized. HA-specific IgG titers increased rapidly after boosting in the offspring of naive but not of vaccinated mothers (Figure 5E). Accordingly, high frequencies of PCs and MBCs were identified in HA-boosted mice born to control mothers, whereas none were observed in the HA-boosted offspring of immune mothers (Figures 5F and 5G).

The unexpected observation that MatAbs drastically affect the GC output, including MBC generation, prompted us to confirm these findings using a different experimental model. Two-week-old pups born to tetanus toxoid (TT)-immunized (or control) mothers were immunized (or not) with TT/alum. In unimmunized pups from immune mothers, TT-specific MatAbs persisted up to

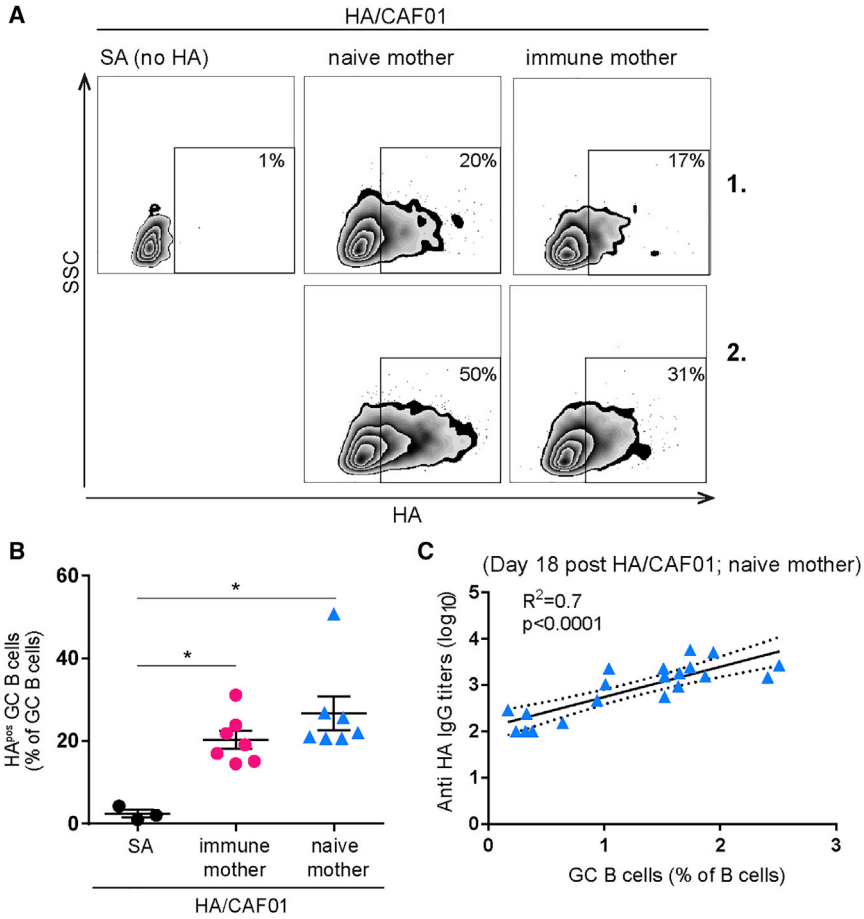

Figure 4. Detection of HA-Specific GC B Cells after a Single Injection of HA/CAF01

(A–C) Neonates born to HA/MF59-immunized or naive mothers were vaccinated with HA/CAF01. Draining LNs were harvested on day 18 after immunization.

(A and B) The frequency of $GL7^+FAS^+$ GC B cells that were able to bind biotinylated HA was assessed by flow cytometry after addition of BV421-conjugated streptavidin. Staining of cells with streptavidin (SA) only in the absence of HA was used to verify the specificity of the binding. Representative plots show frequencies of HA-specific GC B cells in mildly (1) and highly responsive (2) mice (A). Graph shows frequencies of HA-specific GC B cells (B). Dots show values per individual mouse, whereas black lines indicate means ± SEM n = 7 mice/group, Mann-Whitney *U* test: *p < 0.05. Data are representative of at least two independent experiments.

(C) Graph showing the correlation between total GC B cell frequencies and HA-specific IgG antibody responses in neonates born to naive mothers. n = 8 mice/group; data were pooled from at least two independent experiments.

24 weeks after birth (Figure S4A). Again, active immunization did not elicit TT-specific IgG titers in pups from immunized mothers (Figure S4B). TT/alum preferentially induced IgG1 antibodies (Figure S4C), and $IgG_1{}^b$ antibodies were again only detected in immunized pups from naive mothers, confirming total inhibition of antibody responses by high levels of MatAbs (Figure S4D). Vaccinated mice were boosted 12 weeks after prime with TT/PBS to measure B cell recall responses. Again, TT-specific IgG titers did not increase after boosting in the offspring of vaccinated mothers (Figure S4B), and TT-specific PCs and MBCs were only observed in pups immunized in the absence of anti-TT MatAbs (Figures S4E and S4F). Immunization with both TT and HA of pups born to TT-immunized mothers elicited normal primary antibody, PC, and MBC responses to HA, contrasting the full inhibition of TT-specific responses and confirming the antigen specificity of the inhibition mediated by MatAbs (Figures S4G–S4I).

The Level of Maternal Antibodies Present at Priming Determines GC B Cell Differentiation toward PCs and MBCs

In human infants, MatAbs classically inhibit primary antibody responses to vaccination (Markowitz et al., 1996). In most cases, normal booster responses are elicited after MatAbs have waned, suggesting little, if any, interference with MBC induction (Bertley et al., 2004). However, there is clinical evidence that MatAbs depress both primary and secondary antibody responses in young infants vaccinated against measles (Njie-Jobe et al., 2012).

To study the influence of lower MatAb titers on B cell differentiation, we developed a second model in which BALB/c females were immunized twice with HA/PBS instead of HA/MF59 before mating with C57BL/6J males. CB6F1 neonates were then immunized with HA/CAF01 in the presence of lower (3.8 log10 instead of 5 log10) anti-HA IgG MatAb titers. Again, primary antibody responses were fully inhibited by MatAbs (Figure 6A), and HA-specific $IgG1^b$ antibodies were not detected in these pups (data not shown). After HA/PBS boosting, antibody titers increased in all primed mice, although they remained significantly lower and of lower avidity in the offspring of immune than control mothers (Figures 6A and 6B).

Accordingly, both PC (Figure 6C) and MBC (Figure 6D) responses were detected after boosting in immunized mice born to immune mothers, at lower levels than in mice born to naive mothers.

Thus, PC and MBC differentiation during GC responses may be totally abrogated or reduced by various levels of MatAbs, explaining the influence of MatAb titers at the time of immunization on the degree of inhibition of infant antibody responses (Markowitz et al., 1996).

Increasing the TT antigen dose also partially overcame the inhibition of antibody responses to vaccination in neonates born with MatAbs (Figure S5), confirming that the MatAbs/antigen dose ratio at the time of immunization determines the level of inhibition (Siegrist, 2003). Again, antibodies generated in pups from TT-immune mothers were of lower avidity than the ones elicited in control mice (Figure S5C).

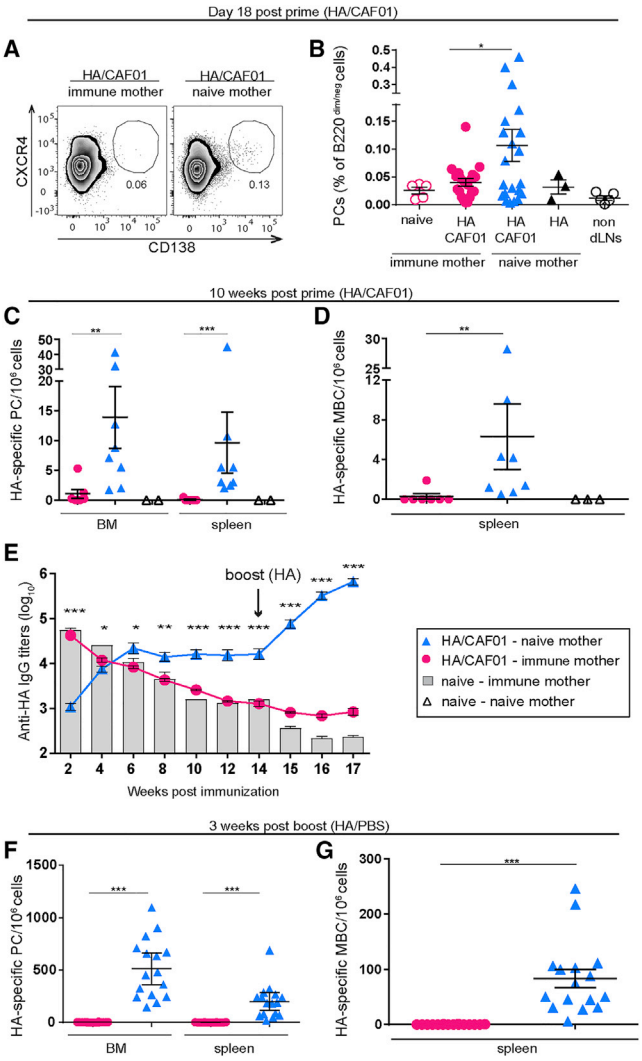

Figure 5. High Titers of Maternal Antibodies Prevent GC B Cell Differentiation toward PCs and MBCs

(A–G) CB6F1 neonates born to HA/MF59-immunized or naive mothers were immunized with HA/CAF01 and boosted 14 weeks later with HA/PBS to measure B cell recall responses. Neonates immunized with HA/PBS or unimmunized served as controls.

(A and B) Cell suspensions from dLNs were analyzed by flow cytometry on day 18 after priming. Representative plots (A) and the graph (B) report the frequencies of $B220^{int/low}CXCR4^{+}CD138^{+}$ PCs for the indicated conditions.

(C and D) Long-lived PCs (C) in the bone marrow (BM) and spleen and (D) MBCs were measured 10 weeks after priming by ELISpot. Data are representative of at least two independent experiments. n = 3–8 mice/group. *$p < 0.05$, **$p < 0.01$, ***$p < 0.001$.

(E) Total IgG titers were assessed at regular intervals. Values represent mean logarithmic titers (log10) of at least six mice per group ± SEM. Statistics show significant differences between HA/CAF01-immunized pups of immune and naive mothers.

(F and G) Long-lived PCs (F) and MBCs (G) 3 weeks after boosting. Dots show values per individual mouse, whereas black lines indicate means ± SEM.

Data were pooled from at least two independent experiments (B, E, F, and G); Student's t test (B) or Mann-Whitney *U* test (C–G).

High Titers of Maternal Antibodies Do Not Affect the GC B Cell Signature Induced by HA/CAF01 in Neonates but Interfere With Post-GC B Cell Differentiation

We next used genome-wide transcriptomics to characterize the influence of MatAbs on GC responses elicited by HA/CAF01 in neonates. Neonates born to HA/MF59-immunized or naive mothers were vaccinated with HA/CAF01, and their dLNs were collected 18 days later to isolate $CD19^{+}B220^{+}GL7^{+}FAS^{+}$ GC B cells and control $CD19^{+}B220^{+}$ $GL7^{neg}FAS^{neg}$ non-GC B cells by flow cytometry cell sorting, according to the gates depicted in Figure 7A. Gene expression analysis was performed by RNA sequencing. We generated a multi-dimensional scaling plot to obtain quantitative estimates of similarity among groups; GC B cells adopted a unique activation and transcriptional state and nicely separated from the rest of the B cells (Figure S6A).

Next we identified the differentially expressed genes (DEGs), defined as those with a significant change in expression (adjusted $p < 0.05$ false discovery rate [FDR]) in GC versus non-GC B cells. Volcano plots illustrate the numbers of significantly downregulated (blue dots) and upregulated (red dots) DEGs in neonates born to naive (Figure S6B) or immune mothers (Figure S6C). Changes reported as being relevant to GC B cell biology in adults (Klein et al., 2003; De Silva and Klein, 2015) were observed in neonates, regardless of whether HA/CAF01 immunization was performed in the presence or absence of MatAbs. The heatmaps illustrate the expression levels of selected GC-related genes, grouped in main categories: cell cycle-related genes, GC-associated surface molecules, transcription factors, apoptosis-related genes, and miscellaneous, with the latter including relevant but unrelated genes (Figure 7B). The GC is a site of intense B cell proliferation and cell death, and the transition of a naive to a GC B cell is associated with dramatic changes in the expression of genes related to cell proliferation and apoptosis (Klein et al., 2003). Accordingly, proliferation-associated genes (e.g., the *CDC* and *CCN* genes) and pro-apoptotic genes (e.g., *Fas* and *Casp3*) were highly expressed in GC B cells, whereas the levels of *Bcl2* and *Nlrp10*, negative regulators of apoptosis, were lower compared with non-GC B cells. Other key changes associated with the GC B cell state following immunization of adults were observed in early life: upregulation of the *Bcl6* and *E2f1* transcription factors, both important for GC formation. *E2f1* induces *Ezh2* expression, which controls G1-to-S phase transition of GC B cells (Béguelin et al., 2017). Downregulation of *Gpr183* allows GC B cell migration to the follicle (Gatto et al., 2009). Downregulation of *S1pr1* and upregulation of *S1pr2* promote confinement of B cells in the GC (Green and Cyster, 2012).

Thus, the canonical changes reflecting the acquisition of a GC B cell phenotype and state after HA/CAF01 neonatal immunization are not affected by even high titers of MatAbs.

To better understand why GC B cells failed to differentiate into MBCs and PCs in vaccinated pups of immune mothers, we next compared GC B cells by RNA sequencing. Prior to antigen-driven activation, resting B cells express IgM or IgD. Within the GC, B cells proliferate at a high rate and undergo class switch recombination (CSR) and somatic hypermutation (SHM). CSR exchanges the Ig heavy-chain (*Ighv*) IgM constant region for those of IgG, IgA, or IgE. The SHM of IgV genes drives affinity maturation through selective expansion of cells with enhanced

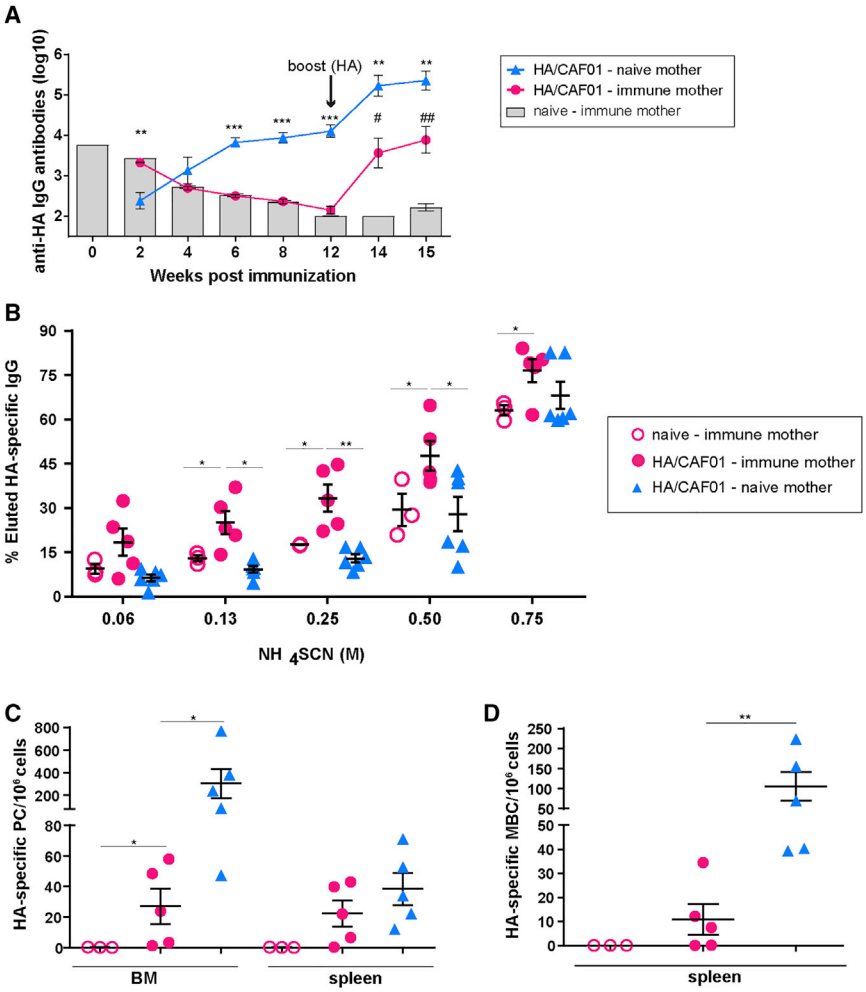

Figure 6. The Level of Maternal Antibodies Present at Priming Determines GC B Cell Differentiation toward PCs and MBCs

(A–D) 1-week-old CB6F1 mice born to HA/PBS-immunized or naive mothers were immunized with HA/CAF01 and boosted 12 weeks later with HA/PBS to measure B cell recall responses. Unimmunized neonates from immune mothers served as controls.

(A) Total IgG titers were measured over time after prime (HA/CAF01) and boost (HA/PBS). Values represent mean logarithmic titers (log10) ± SEM; Mann-Whitney *U* test. Asterisks indicate significant differences between HA/CAF01-immunized pups from immunized and naive mothers: $^{**}p < 0.01$, $^{***}p < 0.001$. # symbols indicate significant differences between HA/CAF01-immunized and naive pups from immune mothers: $^{\#}p < 0.05$, $^{\#\#}p < 0.01$.

(B) The avidity of IgG antibodies was measured 15 weeks after priming (3 weeks after HA boosting) and is represented as percentages of eluted HA-specific antibodies after treatment with increasing concentrations of ammonium thiocyanate (NH_4SCN).

(C and D) Long-lived PCs in the BM and spleen (C) and MBCs (D) were measured 3 weeks after boost by ELISpot. Dots show values per individual mouse, whereas black lines indicate means ± SEM; n = 3–6 mice/group. Data are representative of at least two independent experiments. Mann-Whitney *U* test; $^{*}p < 0.05$, $^{**}p < 0.01$.

antigen binding (Victora and Nussenzweig, 2012), and high affinity drives B cell differentiation toward PCs or MBCs (Kräutler et al., 2017), ensuring the most productive GC output.

Only 39 DEGs distinguished GC B cells elicited in the presence or absence of MatAbs (Figures 7C and 7D). Most were *Ighv* and *Igkv* genes, indicating that GC B cells generated in presence or absence of MatAbs use distinct B cell receptors (BCRs); i.e., they are responding to different epitopes (Figures 7C and 7D).

Significantly lower levels of the *Ighm*, *Ighg2b*, and *Ighg2c* genes and increased levels of *Ighg1* were observed in GC B cells from the offspring of naive mothers, in accordance with the observed antibody responses in this group, predominantly IgG1. Antigen-specific IgM responses were also inhibited in the presence of high levels of MatAbs (Figures S7A and S7B). Additional GC DEGs elicited in the presence of MatAbs included higher levels of *tbx21* (*t-bet*), whose restraint has been shown to be important during an anti-influenza response (Piovesan et al., 2017), and *Cd72*, a negative regulator of B cell responsiveness (Parnes and Pan, 2000), whose suppression is necessary for B cell differentiation. Lower levels of *Nr4a1* (*Nur77*) and *Fosb* were also observed; *Nr4a1* regulates B cell survival and activation (Mayer et al., 2017), whereas *Fos* genes encode leucine zipper proteins that contribute to the AP-1 transcription factor complex (Arguni et al., 2006), which positively regulates terminal differentiation of activated B cells. Lower levels of *Slpi*, which plays a role in regulating the activation of nuclear factor κB (NF-κB) and inflammatory responses (Mulligan et al., 2000), of *Osgin1* and *Capn11*, which regulate apoptosis, and of the *Cystm1* gene, which encodes a protein of the innate immune system-related pathways, all concur to limit B cell differentiation within GC B cells elicited in the presence of MatAbs.

Thus, high MatAb titers do not block B cell priming, as considered previously. They shape GC B cell differentiation, and, thus, limit the generation of PCs and MBCs in a MatAb titer-dependent manner. Major differences in *Ighv* and *Igkv* gene usage indicate that GC B cells elicited in the presence of MatAbs express distinct BCRs; i.e., they bind to distinct epitopes. This could be explained by the masking of immunodominant epitopes by MatAbs and the subsequent restriction of early-life B cell responses to non-immunodominant epitopes failing to drive the affinity-dependent terminal T_{FH} cell/GC B cell differentiation.

DISCUSSION

Although infectious diseases remain a major cause of death in early life (Kollmann et al., 2017), many vaccines are not licensed or require several doses to elicit protection under 6 months of

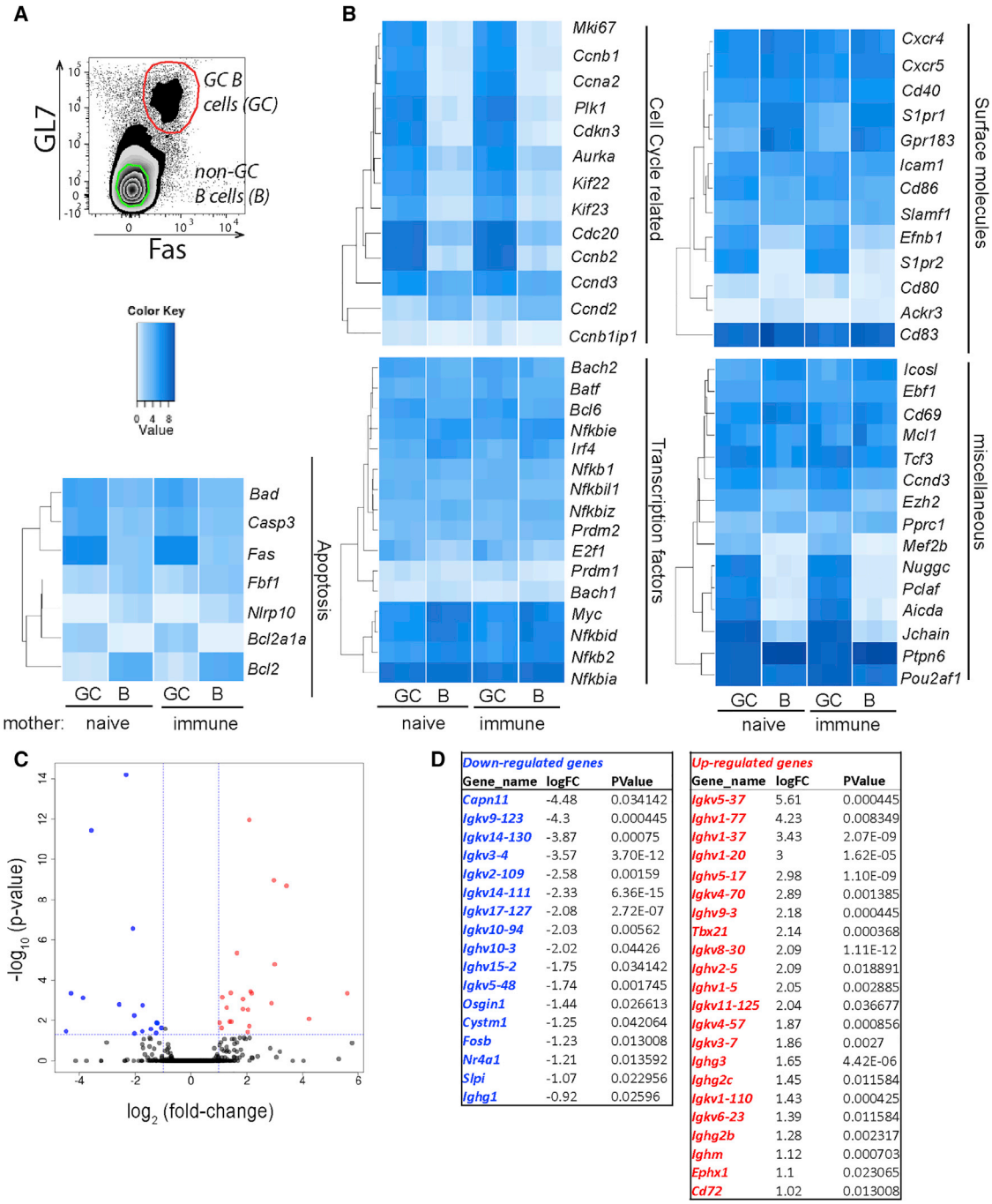

D

Down-regulated genes

Gene_name	logFC	PValue
Capn11	-4.48	0.034142
Igkv9-123	-4.3	0.000445
Igkv14-130	-3.87	0.00075
Igkv3-4	-3.57	3.70E-12
Igkv2-109	-2.58	0.00159
Igkv14-111	-2.33	6.36E-15
Igkv17-127	-2.08	2.72E-07
Igkv10-94	-2.03	0.00562
Ighv10-3	-2.02	0.04426
Ighv15-2	-1.75	0.034142
Igkv5-48	-1.74	0.001745
Osgin1	-1.44	0.026613
Cystm1	-1.25	0.042064
Fosb	-1.23	0.013008
Nr4a1	-1.21	0.013592
Slpi	-1.07	0.022956
Ighg1	-0.92	0.02596

Up-regulated genes

Gene_name	logFC	PValue
Igkv5-37	5.61	0.000445
Ighv1-77	4.23	0.008349
Ighv1-37	3.43	2.07E-09
Ighv1-20	3	1.62E-05
Ighv5-17	2.98	1.10E-09
Igkv4-70	2.89	0.001385
Ighv9-3	2.18	0.000445
Tbx21	2.14	0.000368
Igkv8-30	2.09	1.11E-12
Ighv2-5	2.09	0.018891
Ighv1-5	2.05	0.002885
Igkv11-125	2.04	0.036677
Igkv4-57	1.87	0.000856
Igkv3-7	1.86	0.0027
Ighg3	1.65	4.42E-06
Ighg2c	1.45	0.011584
Igkv1-110	1.43	0.000425
Igkv6-23	1.39	0.011584
Ighg2b	1.28	0.002317
Ighm	1.12	0.000703
Ephx1	1.1	0.023065
Cd72	1.02	0.013008

Figure 7. High Titers of Maternal Antibodies Do Not Affect the GC B Cell Signature Induced by HA/CAF01 in Neonates but Interfere with Post-GC B Cell Differentiation

(A–D) 1-week-old CB6F1 mice born to HA/MF59-immunized or naive mothers were vaccinated with HA/CAF01.

(A) 18 days later, the two inguinal dLNs from 8 pups per group were collected and pooled to isolate sufficient numbers of highly pure (99%) $CD19^+B220^+GL7^+FAS^+$ GC B cells (GC) and control $CD19^+B220^+$ $GL7^{neg}FAS^{neg}$ non-GC B cells (indicated as B) by flow cytometry cell sorting according to the illustrated gates.

(B) Transcriptomic studies were performed by RNA sequencing (RNA-seq). Heatmaps illustrate the expression levels of selected canonical GC genes in log_2 (1+ reads per kilobase per million reads [RPKM]). Results include 3 independent pools of 8 mice per group.

(C) Volcano plot illustrating the numbers of significantly downregulated (blue dots) and upregulated (red dots) genes in GC B cells elicited in the presence compared with the absence of MatAbs.

(D) Tables reporting significantly DEGs in GC B cells elicited in the presence compared with the absence of MatAbs, including gene name, log_2 fold change (FC), and p values.

age. Protection against early-life infections like neonatal tetanus, pertussis, or influenza may thus be best achieved by maternal immunization and transplacental transfer of MatAbs. However, MatAb titers decline with age, reaching titers insufficient for seroprotection while still interfering with infant antigen-specific vaccine responses, generating a transient window of increased vulnerability to infections.

The current concept is that immunization in the presence of MatAbs essentially leaves $CD4^+$ T cells unaffected but prevents B cell activation and, thus, antibody responses (Siegrist, 2003).

Using several neonatal/infant immunization models, we show here (1) that although $CD4^+$ T effector cell responses remain intact, T_{FH} cells prematurely decline and (2) that even high titers of MatAbs do not prevent B cell activation, GC B cell differentiation, and the constitution of *bona fide* GC responses to neonatal immunization. However, MatAbs drastically modulate the GC output by reducing or preventing the generation of PCs and MBCs in a MatAb- and antigen dose-dependent manner.

MatAbs exert their strongest influence on GC B cell differentiation into antibody-secreting PCs; inhibition of antibody responses is exerted even at low MatAb titers (Figure 6A; unpublished data), as observed in human infants (Edwards, 2015). PC generation predominates late in the GC reaction (Weisel et al., 2016), during which B cells do not undergo PC differentiation stochastically; only GC B cells that have acquired a high affinity for the immunizing antigen through successive rounds of differentiation between dark and light zones successfully form PCs (Phan et al., 2006). This affinity maturation process requires continuous T_{FH}/B cell interactions within the GC (Zhang et al., 2016). The normal induction but premature decline of T_{FH} cell responses observed in the vaccinated offspring of immune mothers (Figures 2B–2D) is direct evidence showing that MatAbs influence the late phase of the GC reaction, limiting PC generation.

At low or intermediate titers, MatAbs do not prevent the induction of MBCs, which may be rapidly recalled by a booster dose given after MatAbs waning. MBCs develop early after immunization (Weisel et al., 2016), at a stage during which we observed normal numbers of T_{FH} cells, presuming effective T_{FH}/B cell interactions within the GC. This condition prevails in human infants for most infant vaccines (Bertley et al., 2004). Because microbial exposure also reactivates MBCs and triggers their differentiation into antibody-secreting PCs, their preserved induction/differentiation may contribute to limit the increased vulnerability induced by the presence of MatAbs. High MatAb titers, however, prevent the induction of MBCs, inhibiting anamnestic responses even to late boosters. Thus, MatAbs shape the GC output, interfering first with PC and, subsequently, even with MBC differentiation depending on their level at the time of neonatal/infant immunization.

In addition to these quantitative effects, we observed a profound qualitative influence of MatAbs on the early-life B cell differentiation process. GC B cells elicited by neonatal HA/CAF01 immunization in the presence or absence of MatAbs had similar phenotype and transcriptional profiles, indicating that MatAbs do not block the development of canonical GC B cells. However, although HA/CAF01 mainly induces IgG1 antibodies, a significantly higher level of *Ighm* gene expression was observed in GC B cells elicited in presence of MatAbs, revealing limitations in the CSR, which exchanges the Ig heavy-chain constant region from that encoding IgM to that of IgG1. Furthermore, MatAbs elicited a drastic influence on *Ighv* and *Igkv* gene usage, indicating that B cells that differentiate into GC B cells in the presence or absence of MatAbs express distinct BCRs; i.e., they bind to distinct epitopes of vaccine antigens.

Previous studies revealed that adjuvants influence the immune hierarchy of the immune response (Khurana et al., 2010). Because we used two distinct vaccine adjuvants for mothers (MF59) and pups (CAF01), the full inhibition of primary antibody, PC, and even MBC responses was unexpected. However, we cannot exclude a similar epitope specificity of antibodies elicited by MF59- and CAF01-adjuvanted HA vaccines, enabling MatAbs elicited by HA/MF59 to efficiently mask the immunodominant epitopes recognized by the neonatal B cells induced by HA/CAF01.

GC B cell clones acquiring increased affinity for antigen via SHM are preferentially retained and selectively expanded (Victora and Nussenzweig, 2012; Jacob et al., 1991; Berek et al., 1991), and only high-affinity B cells undergo CSR. Altogether, the observations that GC B cells elicited in presence of MatAbs were fewer, preferably expressed IgM, used distinct *Ighv*/*Igkv* genes than GC B cells of control pups, and failed to differentiate into PCs all suggest that MatAbs impair the affinity maturation process; high-avidity MatAbs (Figures S7C and S7D) binding to immunodominant epitopes may force binding of early-life B cells to non-immunodominant epitopes. These are of lower affinity, limiting their recruitment into the GC and reducing their chance of surviving through the GC selection and PC differentiation processes (Phan et al., 2006).

This hypothesis is supported by the observation that antibody responses generated in the offspring of immune mothers, when observed, are of lower avidity than in control mice (Figures 6B and S5C). Direct evidence of this phenomenon is difficult to obtain, given the paucity of epitope-specific GC B cells elicited early in life, but our experimental findings all concur with the conclusion that MatAbs affect epitope selection by infant B cells.

Epitope masking by MatAbs preventing infant B cell recognition is not a new hypothesis (Getahun and Heyman, 2009; Niewiesk, 2014) and is supported by numerous experiments on antibody feedback regulation (Brüggemann and Rajewsky, 1982; Heyman and Wigzell, 1984; Bergström et al., 2017). Our observations do not exclude a role for steric hindrance or for BCR and FcγRIIB cross-linking blocking activation of some specific B cells (Karlsson et al., 2001; Sinclair et al., 1968). However, they demonstrate that successful activation and differentiation of neonatal and infant B cells into GC B cells do occur, even in the presence of very high titers of MatAbs, which essentially control the B cell fate within the GC and modulate the B cell repertoire in early life.

Beyond their academic interest, these observations have clinical consequences. First, they indicate that clinical trials comparing vaccine responses in infants of immunized or naturally exposed versus non-immunized naive mothers should not only assess the short-term effect but also the long-term influence of MatAbs; the influence on MBC generation and the potential shift of infant B cell responses from immunodominant

to non-immunodominant epitopes are still unknown. Next, they prompt for the evaluation of immunization strategies maximizing the protective efficacy of maternal immunization while minimizing their inhibitory influence on infant B cell responses. This might be achieved by postponing immunization of infants of immunized mothers or providing additional/booster doses at an age at which MatAbs have declined below the interfering threshold. To some extent, this strategy is already empirically used to ensure sufficient antibody responses (i.e., sufficient B cell activation and PC differentiation) to current infant vaccines. Alternatives include planning for a sufficiently high antigen dose to be included in novel infant vaccines when maternal immunization is being considered; for example, against RSV. The use of distinct vaccines in mothers and infants, possibly recruiting distinct B cells into the immunodominant response, is another attractive hypothesis. Last, it appears wise not to aim to induce higher antibody titers in the mother than required for child protection; using adjuvanted influenza, tetanus, or pertussis vaccines in pregnant women should not be considered, given the demonstrated efficacy of non-adjuvanted vaccines inducing lower MatAb titers.

STAR★METHODS

Detailed methods are provided in the online version of this paper and include the following:

- KEY RESOURCES TABLE
- LEAD CONTACT AND MATERIALS AVAILABILITY
  - Materials Availability Statement
- EXPERIMENTAL MODEL AND SUBJECT DETAILS
  - Mice
- METHODS DETAILS
  - Antigens, Adjuvants, and Immunization
  - Enzyme-Linked Immunosorbent Assay (ELISA)
  - Enzyme-Linked Immunospot (ELISpot) Assay
  - Avidity Assay
  - Restimulation of HA-Specific $CD4^+$ T Cells
  - Flow Cytometric Analysis of Lymph Node Cells
  - Flow Cytometry Cell Sorting of Germinal Center B cells
  - Immunohistochemistry
  - RNA Sequencing
  - RNA-seq Data Analysis
- QUANTIFICATION AND STATISTICAL ANALYSIS
- DATA AND CODE AVAILABILITY

SUPPLEMENTAL INFORMATION

Supplemental Information can be found online at https://doi.org/10.1016/j.celrep.2019.07.047.

ACKNOWLEDGMENTS

We acknowledge Novartis Vaccines (a GSK company, Siena, Italy) for providing reagents. We thank Robert Brink, Elodie Mohr, David Pejoski, and Francesco Santoro for helpful discussions; Stephane Grillet, Chantal Tougne, Paola Fontannaz, and Anne Rochat for contributions to the experimental work required for this study; Anthony Joubin for assistance with animal care; and the colleagues at the FACS facility at the University of Geneva. We acknowledge the colleagues at the Genomics platform at the University of Geneva for RNA-seq data generation and analysis. We acknowledge funding to C.-A.S. from the European Union's Seventh Framework Programme (Advanced Immunization Technologies, 280873) and from the Swiss National Science Foundation (310000-111926/1 and 310030-165960).

AUTHOR CONTRIBUTIONS

M.V., P.-H.L., and C.-A.S. designed the research and interpreted the data. M.V., C.S.E., F.A., and B.M.-G. performed the experiments, analyzed data, and/or provided intellectual input. S.L. performed RNA-seq data analysis. D.C. and P.A. provided reagents and intellectual input. M.V. and C.-A.S. wrote the manuscript. All authors reviewed the manuscript.

DECLARATION OF INTERESTS

D.C. and P.A. are co-inventors on patent applications covering CAF01. As employees, D.C. and P.A. have assigned all rights to Statens Serum Institut, a Danish non-profit governmental institute.

Received: March 5, 2019
Revised: July 1, 2019
Accepted: July 15, 2019
Published: August 13, 2019

REFERENCES

Arguni, E., Arima, M., Tsuruoka, N., Sakamoto, A., Hatano, M., and Tokuhisa, T. (2006). JunD/AP-1 and STAT3 are the major enhancer molecules for high Bcl6 expression in germinal center B cells. Int. Immunol. *18*, 1079–1089.

Béguelin, W., Rivas, M.A., Calvo Fernández, M.T., Teater, M., Purwada, A., Redmond, D., Shen, H., Challman, M.F., Elemento, O., Singh, A., and Melnick, A.M. (2017). EZH2 enables germinal centre formation through epigenetic silencing of CDKN1A and an Rb-E2F1 feedback loop. Nat. Commun. *8*, 877.

Benowitz, I., Esposito, D.B., Gracey, K.D., Shapiro, E.D., and Vázquez, M. (2010). Influenza vaccine given to pregnant women reduces hospitalization due to influenza in their infants. Clin. Infect. Dis. *51*, 1355–1361.

Berek, C., Berger, A., and Apel, M. (1991). Maturation of the immune response in germinal centers. Cell *67*, 1121–1129.

Bergström, J.J., Xu, H., and Heyman, B. (2017). Epitope-Specific Suppression of IgG Responses by Passively Administered Specific IgG: Evidence of Epitope Masking. Front. Immunol. *8*, 238.

Bertley, F.M., Ibrahim, S.A., Libman, M., and Ward, B.J. (2004). Measles vaccination in the presence of maternal antibodies primes for a balanced humoral and cellular response to revaccination. Vaccine *23*, 444–449.

Bhutta, Z.A., and Black, R.E. (2013). Global maternal, newborn, and child health–so near and yet so far. N. Engl. J. Med. *369*, 2226–2235.

Borràs, E., Urbiztondo, L., Costa, J., Batalla, J., Torner, N., Plasencia, A., Salleras, L., and Domínguez, À.; Working Group for the Study of Measles Immunity in Children (2012). Measles antibodies and response to vaccination in children aged less than 14 months: implications for age of vaccination. Epidemiol. Infect. *140*, 1599–1606.

Brüggemann, M., and Rajewsky, K. (1982). Regulation of the antibody response against hapten-coupled erythrocytes by monoclonal antihapten antibodies of various isotypes. Cell. Immunol. *71*, 365–373.

Crotty, S. (2011). Follicular helper CD4 T cells (TFH). Annu. Rev. Immunol. *29*, 621–663.

Crowe, J.E., Jr., Firestone, C.Y., and Murphy, B.R. (2001). Passively acquired antibodies suppress humoral but not cell-mediated immunity in mice immunized with live attenuated respiratory syncytial virus vaccines. J. Immunol. *167*, 3910–3918.

Daly, K.A., Scott Giebink, G., Lindgren, B.R., Knox, J., Haggerty, B.J., Nordin, J., Goetz, S., and Ferrieri, P. (2014). Maternal immunization with pneumococcal 9-valent conjugate vaccine and early infant otitis media. Vaccine *32*, 6948–6955.

Davidsen, J., Rosenkrands, I., Christensen, D., Vangala, A., Kirby, D., Perrie, Y., Agger, E.M., and Andersen, P. (2005). Characterization of cationic liposomes based on dimethyldioctadecylammonium and synthetic cord factor from M. tuberculosis (trehalose 6,6′-dibehenate)-a novel adjuvant inducing both strong CMI and antibody responses. Biochim. Biophys. Acta *1718*, 22–31.

De Silva, N.S., and Klein, U. (2015). Dynamics of B cells in germinal centres. Nat. Rev. Immunol. *15*, 137–148.

Edwards, K.M. (2015). Maternal antibodies and infant immune responses to vaccines. Vaccine *33*, 6469–6472.

Englund, J.A., Anderson, E.L., Reed, G.F., Decker, M.D., Edwards, K.M., Pichichero, M.E., Steinhoff, M.C., Rennels, M.B., Deforest, A., and Meade, B.D. (1995). The effect of maternal antibody on the serologic response and the incidence of adverse reactions after primary immunization with acellular and whole-cell pertussis vaccines combined with diphtheria and tetanus toxoids. Pediatrics *96*, 580–584.

Gatto, D., Paus, D., Basten, A., Mackay, C.R., and Brink, R. (2009). Guidance of B cells by the orphan G protein-coupled receptor EBI2 shapes humoral immune responses. Immunity *31*, 259–269.

Getahun, A., and Heyman, B. (2009). Studies on the mechanism by which antigen-specific IgG suppresses primary antibody responses: evidence for epitope masking and decreased localization of antigen in the spleen. Scand. J. Immunol. *70*, 277–287.

Giles, M.L., Krishnaswamy, S., and Wallace, E.M. (2018). Maternal immunisation: What have been the gains? Where are the gaps? What does the future hold? F1000Res. *7*, F1000 Faculty Rev-1733.

Green, J.A., and Cyster, J.G. (2012). S1PR2 links germinal center confinement and growth regulation. Immunol. Rev. *247*, 36–51.

Heyman, B., and Wigzell, H. (1984). Immunoregulation by monoclonal sheep erythrocyte-specific IgG antibodies: suppression is correlated to level of antigen binding and not to isotype. J. Immunol. *132*, 1136–1143.

Jacob, J., Kelsoe, G., Rajewsky, K., and Weiss, U. (1991). Intraclonal generation of antibody mutants in germinal centres. Nature *354*, 389–392.

Jones, C., Pollock, L., Barnett, S.M., Battersby, A., and Kampmann, B. (2014). The relationship between concentration of specific antibody at birth and subsequent response to primary immunization. Vaccine *32*, 996–1002.

Kachikis, A., and Englund, J.A. (2016). Maternal immunization: Optimizing protection for the mother and infant. J. Infect *72*, S83–S90.

Karlsson, M.C., Getahun, A., and Heyman, B. (2001). FcgammaRIIB in IgG-mediated suppression of antibody responses: different impact in vivo and in vitro. J. Immunol. *167*, 5558–5564.

Khurana, S., Chearwae, W., Castellino, F., Manischewitz, J., King, L.R., Honorkiewicz, A., Rock, M.T., Edwards, K.M., Del Giudice, G., Rappuoli, R., and Golding, H. (2010). Vaccines with MF59 adjuvant expand the antibody repertoire to target protective sites of pandemic avian H5N1 influenza virus. Sci. Transl. Med. *2*, 15ra5.

Kim, D., Huey, D., Oglesbee, M., and Niewiesk, S. (2011). Insights into the regulatory mechanism controlling the inhibition of vaccine-induced seroconversion by maternal antibodies. Blood *117*, 6143–6151.

Klein, U., Tu, Y., Stolovitzky, G.A., Keller, J.L., Haddad, J., Jr., Miljkovic, V., Cattoretti, G., Califano, A., and Dalla-Favera, R. (2003). Transcriptional analysis of the B cell germinal center reaction. Proc. Natl. Acad. Sci. USA *100*, 2639–2644.

Kollmann, T.R., Kampmann, B., Mazmanian, S.K., Marchant, A., and Levy, O. (2017). Protecting the Newborn and Young Infant from Infectious Diseases: Lessons from Immune Ontogeny. Immunity *46*, 350–363.

Kräutler, N.J., Suan, D., Butt, D., Bourne, K., Hermes, J.R., Chan, T.D., Sundling, C., Kaplan, W., Schofield, P., Jackson, J., et al. (2017). Differentiation of germinal center B cells into plasma cells is initiated by high-affinity antigen and completed by Tfh cells. J. Exp. Med. *214*, 1259–1267.

Kurikka, S., Käyhty, H., Peltola, H., Saarinen, L., Eskola, J., and Mäkelä, P.H. (1995). Neonatal immunization: response to Haemophilus influenzae type b-tetanus toxoid conjugate vaccine. Pediatrics *95*, 815–822.

Liao, Y., Smyth, G.K., and Shi, W. (2014). featureCounts: an efficient general purpose program for assigning sequence reads to genomic features. Bioinformatics *30*, 923–930.

Lin, S.M., Zhi, Y., Ahn, K.B., Lim, S., and Seo, H.S. (2018). Status of group B streptococcal vaccine development. Clin. Exp. Vaccine Res. *7*, 76–81.

Macdonald, R.A., Hosking, C.S., and Jones, C.L. (1988). The measurement of relative antibody affinity by ELISA using thiocyanate elution. J. Immunol. Methods *106*, 191–194.

Maertens, K., Tran, T.M.P., Hens, N., Van Damme, P., and Leuridan, E. (2017). Effect of Prepregnancy Pertussis Vaccination in Young Infants. J. Infect. Dis. *215*, 1855–1861.

Markowitz, L.E., Albrecht, P., Rhodes, P., Demonteverde, R., Swint, E., Maes, E.F., Powell, C., and Patriarca, P.A.; Kaiser Permanente Measles Vaccine Trial Team (1996). Changing levels of measles antibody titers in women and children in the United States: impact on response to vaccination. Pediatrics *97*, 53–58.

Mastelic Gavillet, B., Eberhardt, C.S., Auderset, F., Castellino, F., Seubert, A., Tregoning, J.S., Lambert, P.H., de Gregorio, E., Del Giudice, G., and Siegrist, C.A. (2015). MF59 Mediates Its B Cell Adjuvanticity by Promoting T Follicular Helper Cells and Thus Germinal Center Responses in Adult and Early Life. J. Immunol. *194*, 4836–4845.

Mayer, C.T., Gazumyan, A., Kara, E.E., Gitlin, A.D., Golijanin, J., Viant, C., Pai, J., Oliveira, T.Y., Wang, Q., Escolano, A., et al. (2017). The microanatomic segregation of selection by apoptosis in the germinal center. Science *358*, eaao2602.

Mazur, N.I., Higgins, D., Nunes, M.C., Melero, J.A., Langedijk, A.C., Horsley, N., Buchholz, U.J., Openshaw, P.J., McLellan, J.S., Englund, J.A., et al.; Respiratory Syncytial Virus Network (ReSViNET) Foundation (2018). The respiratory syncytial virus vaccine landscape: lessons from the graveyard and promising candidates. Lancet Infect. Dis. *18*, e295–e311.

Mulligan, M.S., Lentsch, A.B., Huber-Lang, M., Guo, R.F., Sarma, V., Wright, C.D., Ulich, T.R., and Ward, P.A. (2000). Anti-inflammatory effects of mutant forms of secretory leukocyte protease inhibitor. Am. J. Pathol. *156*, 1033–1039.

Niewiesk, S. (2014). Maternal antibodies: clinical significance, mechanism of interference with immune responses, and possible vaccination strategies. Front. Immunol. *5*, 446.

Njie-Jobe, J., Nyamweya, S., Miles, D.J., van der Sande, M., Zaman, S., Touray, E., Hossin, S., Adetifa, J., Palmero, M., Burl, S., et al. (2012). Immunological impact of an additional early measles vaccine in Gambian children: responses to a boost at 3 years. Vaccine *30*, 2543–2550.

Parnes, J.R., and Pan, C. (2000). CD72, a negative regulator of B-cell responsiveness. Immunol. Rev. *176*, 75–85.

Phan, T.G., Paus, D., Chan, T.D., Turner, M.L., Nutt, S.L., Basten, A., and Brink, R. (2006). High affinity germinal center B cells are actively selected into the plasma cell compartment. J. Exp. Med. *203*, 2419–2424.

Pihlgren, M., Tougne, C., Schallert, N., Bozzotti, P., Lambert, P.H., and Siegrist, C.A. (2003). CpG-motifs enhance initial and sustained primary tetanus-specific antibody secreting cell responses in spleen and bone marrow, but are more effective in adult than in neonatal mice. Vaccine *21*, 2492–2499.

Piovesan, D., Tempany, J., Di Pietro, A., Baas, I., Yiannis, C., O'Donnell, K., Chen, Y., Peperzak, V., Belz, G.T., Mackay, C.R., et al. (2017). c-Myb Regulates the T-Bet-Dependent Differentiation Program in B Cells to Coordinate Antibody Responses. Cell Rep. *19*, 461–470.

Robinson, M.D., McCarthy, D.J., and Smyth, G.K. (2010). edgeR: a Bioconductor package for differential expression analysis of digital gene expression data. Bioinformatics *26*, 139–140.

Siegrist, C.A. (2003). Mechanisms by which maternal antibodies influence infant vaccine responses: review of hypotheses and definition of main determinants. Vaccine *21*, 3406–3412.

Siegrist, C.A., Barrios, C., Martinez, X., Brandt, C., Berney, M., Córdova, M., Kovarik, J., and Lambert, P.H. (1998a). Influence of maternal antibodies on vaccine responses: inhibition of antibody but not T cell responses allows

successful early prime-boost strategies in mice. Eur. J. Immunol. *28*, 4138–4148.

Siegrist, C.A., Córdova, M., Brandt, C., Barrios, C., Berney, M., Tougne, C., Kovarik, J., and Lambert, P.H. (1998b). Determinants of infant responses to vaccines in presence of maternal antibodies. Vaccine *16*, 1409–1414.

Sinclair, N.R., Lees, R.K., and Elliott, E.V. (1968). Role of the Fc fragment in the regulation of the primary immune response. Nature *220*, 1048–1049.

Victora, G.D., and Nussenzweig, M.C. (2012). Germinal centers. Annu. Rev. Immunol. *30*, 429–457.

Vinuesa, C.G., Linterman, M.A., Goodnow, C.C., and Randall, K.L. (2010). T cells and follicular dendritic cells in germinal center B-cell formation and selection. Immunol. Rev. *237*, 72–89.

Vono, M., Eberhardt, C.S., Mohr, E., Auderset, F., Christensen, D., Schmolke, M., Coler, R., Meinke, A., Andersen, P., Lambert, P.H., et al. (2018). Overcoming the Neonatal Limitations of Inducing Germinal Centers through Liposome-Based Adjuvants Including C-Type Lectin Agonists Trehalose Dibehenate or Curdlan. Front. Immunol. *9*, 381.

Weeratna, R.D., Brazolot Millan, C.L., McCluskie, M.J., Siegrist, C.A., and Davis, H.L. (2001). Priming of immune responses to hepatitis B surface antigen in young mice immunized in the presence of maternally derived antibodies. FEMS Immunol. Med. Microbiol. *30*, 241–247.

Weisel, F.J., Zuccarino-Catania, G.V., Chikina, M., and Shlomchik, M.J. (2016). A Temporal Switch in the Germinal Center Determines Differential Output of Memory B and Plasma Cells. Immunity *44*, 116–130.

Zhang, Y., Garcia-Ibanez, L., and Toellner, K.M. (2016). Regulation of germinal center B-cell differentiation. Immunol. Rev. *270*, 8–19.

STAR★METHODS

KEY RESOURCES TABLE

REAGENT or RESOURCE	SOURCE	IDENTIFIER
Antibodies		
goat anti-Mouse IgG, HRP	Invitrogen	Cat# A16072; RRID: AB_2534745
rat Anti-Mouse IgG1, HRP	BD PharMingen	Cat# 559626; RRID: AB_397292
biotin mouse anti-mouse IgG1b	BD PharMingen	Cat# 553533; RRID: AB_394903
Goat anti-mouse IgM, HRP	ThermoFischer	Cat# 62-6820; RRID: AB_138470
anti-mouse CD28	BD PharMingen	Cat# 553295; RRID: AB_394764
anti-mouse CD49d	BD PharMingen	Cat# 553313; RRID: AB_394776
anti-mouse CD3e	BD PharMingen	Cat# 553057; RRID: AB_394590
PerCp-Cy5.5 anti-mouse CD4	BD PharMingen	Cat# 550954; RRID: AB_2636402
APC/Cy7 anti-mouse CD44	Biolegend	Cat# 103028; RRID: AB_830785
Alexa 700 anti-mouse CD3	BD PharMingen	Cat# 561388; RRID: AB_10642588
APC anti-mouse IFN-γ	BD PharMingen	Cat# 554413; RRID: AB_398551
PE anti-mouse IL-17	BioLegend	Cat# 506904; RRID: AB_315464
Alexa Fluor 488 anti-mouse IL-2	BD PharMingen	Cat# 557725; RRID: AB_396833
eFluor 450 anti-mouse IL-13	Invitrogen	Cat# 48-7133-82; RRID: AB_11219690
BV421 anti-mouse IL-4	BioLegend	Cat# 504119; RRID: AB_10896945
purified anti-mouse CXCR5	BD PharMingen	Cat# 551961; RRID: AB_394302
FITC anti-rat IgG	SouthernBiotech	Cat# 3052-02; RRID: AB_2795844
PE anti-mouse PD-1	Invitrogen	Cat# 12-9985-82; RRID: AB_466295
biotin anti-mouse CD95 (Fas)	Invitrogen	Cat# 13-0951-81; RRID: AB_466544
biotin anti-mouse Ly-6G/Ly-6C	Invitrogen	Cat# 13-5931-85; RRID: AB_466801
biotin anti-mouse TER-119/Erythroid Cells	Invitrogen	Cat# 13-5921-82; RRID: AB_466797
PerCP-eFluor 710 anti-mouse CXCR4 (CD184)	Invitrogen	Cat# 46-9991-82; RRID: AB_10670489
PE-CF594 anti-mouse B220	BD PharMingen	Cat# 562290; RRID: AB_11151901
biotin anti-mouse CD11b	BD PharMingen	Cat# 553309; RRID: AB_394773
Alexa Fluor 488 anti-mouse GL7	BioLegend	Cat# 144612; RRID: AB_2563285
PE/Cy7 anti-mouse TCR β	BioLegend	Cat# 109222; RRID: AB_893625
PE/Cy7 anti-mouse ICOS	BioLegend	Cat# 313520; RRID: AB_10643411
APC/Cy7 anti-mouse CD8a	BioLegend	Cat# 100714; RRID: AB_312753
BV421 anti-mouse CD138	BioLegend	Cat# 142508; RRID: AB_11203544
Pacific Blue anti-mouse CD4	BioLegend	Cat# 100428; RRID: AB_493647
BV510 anti-mouse B220	BioLegend	Cat# 103248; RRID: AB_2650679
BUV395 anti-mouse B220	BD PharMingen	Cat# 563793; RRID: AB_2738427
PE-Cy7 anti-mouse CD19	BD PharMingen	Cat# 552854; RRID: AB_394495
BV510 anti-mouse CD19	BD PharMingen	Cat# 562956; RRID: AB_2737915
PE anti-mouse CD95 (Fas)	Invitrogen	Cat# 12-0951-81; RRID: AB_465788
PECy7 anti-mouse CD11b	BD PharMingen	Cat# 561098; RRID: AB_2033994
PECy7 anti-mouse TCR β	BD PharMingen	Cat# 560729; RRID: AB_1937310
APC anti-mouse TCR β	Invitrogen	Cat# 17-5961-82; RRID: AB_469481
Alexa Fluor 647 anti-mouse Bcl6	BD PharMingen	Cat# 561525; RRID: AB_10898007
Chemicals, Peptides, and Recombinant Proteins		
Biotin- H1N1 A/California/7/2009	Sino Biological	Cat# 11085-V08H (biotinylated under request)
Streptavidin HRP	BD PharMingen	Cat# 554066
Streptavidin BV421	BD PharMingen	Cat# 563259

(*Continued on next page*)

Continued

REAGENT or RESOURCE	SOURCE	IDENTIFIER
R848	Chemdea	Cat# CD0271
Recombinant human IL-2	Peprotech	Cat# 200-02
Brefeldin A	Sigma-Aldrich	Cat# 20350-15-6
FcR Blocking Reagent, mouse	Miltenyi Biotec	Cat# 130-092-575
Normal Rat Serum	Invitrogen	Cat# 10710C
Critical Commercial Assays		
Live/Dead Fixable Aqua Stain Kit	ThermoFisher	Cat# L34957
Live/Dead Fixable Near-IR Stain Kit	ThermoFisher	Cat# L10119
Fixation/Permeabilization Solution Kit	BD Cytofix/Cytoperm	Cat# 554714
EasySep Mouse B Cell Isolation Kit	STEMCELL	Cat# 19854
RNeasy Mini Kit	QIAGEN	Cat# 74104
SMARTer Ultra Low RNA kit	Clontech (Takara)	Cat# 634936
Foxp3/Transcription Factor Staining Buffer Set	eBioscience	Cat# 00-5523-00
Deposited Data		
Raw and analyzed RNaseq data	This paper	GEO: GSE126015
Experimental Models: Organisms/Strains		
BALB/c OlaHsd female mice	Envigo	N/A
C57BL/6J OlaHsd male mice	Envigo	N/A
CB6F1 mice	Bred in-house	N/A
Software and Algorithms		
FacsDiva	BD Biosciences	http://www.bdbiosciences.com/en-us/instruments/research-instruments/research-software/flow-cytometry-acquisition/facsdiva-software
FlowJo	FlowJo	https://www.flowjo.com/solutions/flowjo/downloads
Prism	GraphPad	https://www.graphpad.com/scientific-software/prism/
FastQC	Babraham Bioinformatics	https://www.bioinformatics.babraham.ac.uk/projects/fastqc/
featureCounts	Bioconductor	Liao et al., 2014
edgeR	Bioconductor	Robinson et al., 2010
R	R Foundation	https://www.r-project.org/
STAR	GitHub	https://github.com/alexdobin/STAR/releases
Other		
H1N1 A/California/7/2009	Former Novartis Vaccines (a GSK Company)	N/A
CAF01	Statens Serum Institut	Davidsen et al., 2005
MF59	Former Novartis Vaccines (a GSK Company)	N/A
Tetanus Toxoid	Sanofi Pasteur	N/A
Alum	Sanofi Pasteur	N/A
Infanrix (DTPa)	GSK	N/A

LEAD CONTACT AND MATERIALS AVAILABILITY

Further information and requests for resources and reagents should be directed to and will be fulfilled by the Lead Contact, Maria Vono (maria.vono@unige.ch)

Materials Availability Statement

This study did not generate new unique reagents.

EXPERIMENTAL MODEL AND SUBJECT DETAILS

Mice

BALB/c OlaHsd females and C57BL/6J OlaHsd males were purchased from Envigo (Horst, the Netherlands) and were crossed to produce F1 CB6F1 mice, both female and male neonatal mice were used in the experiments. Mice were bred in pathogen-free animal facilities in accordance with local guidelines. All experiments were approved by the Geneva veterinary office and conducted under relevant Swiss and European guidelines.

METHODS DETAILS

Antigens, Adjuvants, and Immunization

We used a monovalent purified subunit influenza HA vaccine from H1N1 A/California/7/2009.

In the Influenza models, groups of 5 to 8 BALB/c OlaHsd females were immunized intramuscularly (i.m.) with HA (1 μg) mixed 1:1 (v/v) with MF59 (5% squalene, 0.5% Tween 80, and 0.5% Span 85 in citrate buffer [v/v]) (Novartis Vaccines) or with PBS, twice (day 0 and 21) prior to breeding.

Groups of 5 to 8 CB6F1 neonates (1 week-old) were immunized subcutaneously (s. c.) with HA (1 μg) in PBS or CAF01 (250 μg DDA/ 50 μg TDB, Statens Serum Institut, Copenhagen, Denmark). Groups of neonates received CAF01 only as additional control.

In the tetanus toxoid model, BALB/c females were immunized as above with 1/10 of a human dose of Infanrix® (diphtheria-tetanus-acellular pertussis (DTPa) on aluminum hydroxide, GlaxoSmithKline, Rixensart, Belgium). Groups of 5 to 8 CB6F1 pups were immunized i.m. at 2 weeks of age with the indicated doses (Lf 0.025 or Lf 0.05) of tetanus toxoid (TT, Sanofi Pasteur, Lyon, France) adsorbed to aluminum hydroxide (alum; 0.5 mg per mouse; Sanofi Pasteur). For experiments with TT-HA, groups of 3 to 5 CB6F1 pups were immunized i.m. at 2 weeks of age with both TT (Lf 0.025) and HA (1 μg) adsorbed to aluminum hydroxide (0.5 mg per mouse).

For experiments of adoptive transfer, HA-specific hyperimmune serum (4.6 log10 IgG titers), generated in adult mice, was transferred (100 μl; intraperitoneal injection (IP)) in neonatal mice 24h prior to immunization with HA/CAF01.

Enzyme-Linked Immunosorbent Assay (ELISA)

Titration of Ag-specific total IgG and IgG1 titers was performed by ELISA on individual serum samples as previously described (Mastelic Gavillet et al., 2015; Pihlgren et al., 2003). IgG1b titers were measured similarly, except that a biotin mouse anti-mouse IgG1b antibody was used followed by streptavidin-HRP (both from BD Biosciences). IgM antibodies were measured similarly by using a goat anti-mouse IgM antibody, HRP conjugate (ThermoFischer). Plates were coated with the same antigen (HA or TT) used for immunization.

Enzyme-Linked Immunospot (ELISpot) Assay

HA-specific PCs were quantified by direct *ex vivo* ELISpot assay using 96-well multiscreen HA nitrocellulose filtration plates (Millipore) coated with 50 μL of HA (4 μg/ml) in PBS, the same HA protein used for immunization. As positive control for total IgG-secreting cells, 2 wells per plate were coated with a goat anti-mouse IgG (Invitrogen). The plates were incubated overnight at 4°C, washed twice in PBS, and blocked with RPMI (GIBCO) plus 10% (v/v) Fetal Calf Serum (FCS; Bioconcept). The plates were washed with PBS and cell suspensions were added at an initial number of $4x10^6$ (bone-marrow) or $2x10^6$ (spleen), followed by 1:2 serial dilutions in RPMI/ 10% (v/v) FCS.

The plates were incubated at 37°C, 5% CO_2 for 5 h prior to washing with PBS containing 0.1% (v/v) Tween (PBS-T). 100 μL of goat anti-mouse IgG- HRP conjugated antibody (Invitrogen) diluted 1:1000 in PBS-T containing 1% (v/v) FCS was added and the plates were incubated overnight at 4°C. Plates were first washed with PBS-T and then with PBS. Detection was performed by adding 100 μL of 3-amino-9-ethylcarbazole substrate buffer for 30 min in the dark until spots appeared. The reaction was stopped by thorough washing with cold tap water and air-dried. Spots were counted by eye under the microscope.

MBCs were detected using a modification of the PC ELISpot. In brief, $2x10^7$ splenocytes were transferred in cell culture flask T25 (Nunc) together with 10^7 irradiated (1200 rad) naive congenic splenocytes and rested overnight. Cells were stimulated for 5 days with a combination of R848 (0.5 μg/ml; Chemdea) and IL-2 (5 ng/ml; Peprotech), harvested, washed with RPMI medium and counted. Cell suspensions were added to 96-wells multiscreen HA nitrocellulose filtration plates coated with influenza HA at an initial number of 10^7 cells, followed by eight 2-fold serial dilutions. The ELISpot assay was then performed as described above.

TT-specific PCs and MBCs were quantified similarly, except that plates were coated with 50 μL of TT (9.48 Lf/ml) in PBS.

Avidity Assay

Avidity was measured by an ELISA elution assay as the overall strength of binding between antibody and antigen, using plates incubated for 15 min with increasing concentration of ammonium thiocyanate (NH4SCN) from 0 to 1.5 M in the HA model and from 0 to 3 M in the TT model, according to a well-established method (Macdonald et al., 1988). Antibody avidity was defined as the amount (percentage) of antibody eluted for each increment of NH_4SCN concentration.

Restimulation of HA-Specific CD4$^+$ T Cells

Groups of 5 – 8 mice were sacrificed at day 12 after immunization and spleens were collected to assess the frequency and phenotype of HA-specific CD4$^+$CD44$^+$ T cells.

Intracellular cytokine production was assessed on 4x10^6 splenocytes/well in the presence of anti-CD28, anti-CD49d (both 1 μg/ml, BD Pharmigen), and HA protein (1 μg/ml). Unstimulated or anti-CD3 (1 μg/ml; BD PharMingen) treated cells were used as negative and positive controls, respectively.

Cells were cultured overnight prior to adding Brefeldin A (BFA, 5 μg/ml, Sigma-Aldrich) for the last 4 h. Cells were washed in PBS, labeled with Live/Dead Fixable Aqua Stain Kit (ThermoFisher) and incubated with FcR blocking (Miltenyi Biotec). Surface staining was performed with the following monoclonal antibodies: AF700 anti-CD3, PerCP-Cy5.5 anti-CD4 (both from BD PharMingen) and APC-Cy7 anti-CD44 (Biolegend). Cells were fixed, permeabilized with the Fixation/Permeabilization Solution Kit (BD Cytofix/Cytoperm) and stained intracellularly with APC anti- IFN-γ, AF488 anti-IL-2 (both from BD PharMingen), eFluor 450 anti-IL-13 (Invitrogen), A450 anti-IL-4 and PE anti-IL-17 (both from Biolegend). Samples were acquired on a Gallios cytometer (Beckman Coulter) and the generated data analyzed using FlowJo Software (Tree Star).

Flow Cytometric Analysis of Lymph Node Cells

Cells from the two draining LNs of each mouse were pooled and stained with fluorescently labeled antibodies to B220, and CD11b (all from BD PharMingen), FAS (CD95), PD-1, Ter119, Ly-6G/Ly-6C, CXCR4 (all from Invitrogen), GL7, TCR-β, CD4, CD8, CD138, and ICOS (all from BioLegend). CXCR5 staining was performed using purified anti-CXCR5 (BD PharMingen), followed by FITC anti-rat IgG (Southern Biotech), and normal rat serum (Invitrogen). Intracellular Bcl6 staining was performed by using the Foxp3 transcription factor buffer set (eBioscience) followed by an anti-Bcl6 antibody (BD PharMingen). The amount of live cells in samples was determined by using a Live/Dead viability kit (Thermo Fischer Scientific). To determine antigen specificity, cells were incubated with 20 μg/ml biotinylated HA (Sino Biological) and subsequently with BV421-conjugated streptavidin (BD PharMingen).

The stained cells were analyzed using a Gallios cytometer (Beckman Coulter) or a BD LSRFortessa and the generated data analyzed using FlowJo Software (Tree Star).

Flow Cytometry Cell Sorting of Germinal Center B cells

The 2 inguinal draining LNs were collected 18 days after neonatal immunization, samples from each group were pooled and B cells were enriched by using the EasySep Mouse B Cell Isolation Kit (STEMCELL). Cells were stained with the following antibodies: AF488 anti- GL7, BV510 anti- B220 (BioLegend), PE-Cy7 anti- CD19 (BD PharMingen) PE anti- FAS, and APC anti- TCR β (Invitrogen). B220$^+$CD19$^+$GL7$^+$FAS$^+$ GC B cells (purity $\geq$ 99%) and B220$^+$CD19$^+$GL7^{neg}FAS^{neg} non-GC B cells were simultaneously isolated from the enriched B cells by flow-cytometry cell sorting using a MoFlo® Astrios flow cytometer (Beckman Coulter).

Immunohistochemistry

The draining LNs of immunized mice were stained and quantified as previously described for GC detection (Mastelic Gavillet et al., 2015). Sections were visualized and photographed with a Zeiss LSM700 confocal microscope (objective: 20x). Images were acquired with Zeiss LSM image browser software (Zeiss).

RNA Sequencing

Total RNA was extracted from sorted cells using the RNeasy Mini Kit (QIAGEN, Germany) following the manufacturer's instructions. RNA concentration and integrity were assessed with a Bioanalyzer (Agilent Technologies). The SMARTer Ultra Low RNA kit (Clontech) was used for reverse transcription and cDNA amplification according to the manufacturer's specifications, starting with 10 ng of total RNA as input. 200 pg of cDNA were used for library preparation using the Nextera XT kit from Illumina. Library molarity and quality was assessed with the Qubit and Tapestation using a DNA High sensitivity chip (Agilent Technologies). Libraries were pooled and loaded at 2 nM for clustering on a single-read Illumina flow cell. Reads of 50 bases were generated using the TruSeq SBS chemistry on an Illumina HiSeq 4000 sequencer.

Three independent biological replicates were analyzed for each condition. Sequencing quality was checked and approved via the FastQC software. FastQ reads were mapped to the ENSEMBL reference genome (GRCm38.89) using STAR (version 2.4.0j) with standard settings, except that any reads mapping to more than one location on the genome (ambiguous reads) were discarded (m = 1). The RNA-seq data have been deposited to the Gene Expression Omnibus (GEO) under accession number GSE126015.

RNA-seq Data Analysis

The model used to quantify reads per gene considers all annotated exons of all annotated protein coding isoforms of a gene to create a unique gene where the genomic region of all exons are considered coming from the same RNA molecule and merged together.

All reads overlapping the exons of each unique gene model were reported using featureCounts (version 1.4.6-p1). Gene expressions were reported as raw counts and normalized in RPKM in order to filter out genes with low expression value (1 RPKM) before calling for differentially expressed genes. Library size normalizations and differential gene expression calculations were performed using the package edgeR (Robinson et al., 2010) designed for the R software. Only genes having a significant fold-change (Benjamini-Hochberg corrected p value < 0.05) were considered for the rest of the RNA-seq analysis.

QUANTIFICATION AND STATISTICAL ANALYSIS

Data were analyzed using Prism 7.0 (GraphPad Software) and presented as specified in figure legends. Difference between groups was analyzed as described in figure legends. p values less than 0.05 were considered statistically significant.

DATA AND CODE AVAILABILITY

The RNA-seq data generated during this study are available at the Gene Expression Omnibus under accession number GSE126015.